New Horizons of Time-Domain Astronomy
Proceedings IAU Symposium No. 285, 2011
R.E.M. Griffin, R.J. Hanisch & R. Seaman, eds.

doi:10.1017/S1743921312000610

Gravitational Microlensing

Ł. Wyrzykowski[1,2], M. Moniez[3], K. Horne[4] and R. Street[5]

[1]Institute of Astronomy The Observatories, Cambridge, CB3 0HA, UK

[2]Warsaw University Astronomical Observatory, 00-478 Warszawa, Poland
email: wyrzykow@ast.cam.ac.uk, lw@astrouw.edu.pl

[3]Laboratoire de l'Accélérateur Linéaire, IN2P3-CNRS, Université de Paris-Sud, 91898 Orsay Cedex, France

[4]SUPA Physics & Astronomy, University of St Andrews, KY16 9NS, Scotland

[5]LCOGT, 6740 Cortona Drive, Suite 102, Goleta, CA 93117, USA

Abstract. Gravitational microlensing is a well established and unique field of time-domain astrophysics. For two decades microlensing surveys have been regularly observing millions of stars to detect elusive events that follow a characteristic Paczyński lightcurve. This workshop reviewed the current state of the field, and covered the major topics related to microlensing: searches for extrasolar planets, and studies of dark matter. There were also discussions of issues relating to the organisation of follow-up observations for microlensing, as well as serendipitous scientific outcomes resulting from extensive microlensing data.

Keywords. gravitational microlensing—planets—dark matter—variable stars

---

1. Extrasolar Planets and the Future of Microlensing (KH)

Microlensing happens when a compact object passes near the line of sight to a distant star, causing bending of the light rays and thus magnifying and forming multiple images of the distant source. On the scale of the Galaxy it is observed as a temporary brightening of a star, the light curve following a unique shape known as the "Paczyński lightcurve". If a lensing star harbours a planet, the curve may exhibit a very short blip, a flash or dip, whose duration is of the order of hours to days, depending on the mass ratio of the planet and the star. A suitably high observing cadence is necessary to detect planets in that way.

Thus far, combining the efforts of two wide-angle surveys (OGLE, MOA) and a number of follow-up networks (PLANET, μFUN, RoboNet, MiNDSTeP), some 13 planets have been found, mostly in large (0.5–5 AU) orbits, and with masses ranging from a few Earths to a few Jupiters. Selected highlights among these cool planet detections are:

OGLE-2005-BLG-071 : a cool Super-Jupiter of about 3 M_J at 2 or 4 AU, found as a 3-day anomaly at high magnification (Udalski *et al.* 2005),

OGLE-2005-BLG-390 : a small rock/ice planet of about 6 $M_\oplus$ at 2.9 AU, found as a 12-hour anomaly at low magnification (Beaulieu *et al.* 2006),

OGLE-2006-BLG-109 : a half-scale Solar System analogue hosting two planets with mass ratios and orbit sizes similar to Jupiter and Saturn, found from a long complex anomaly (Gaudi *et al.* 2008),

MOA-2009-BLG-266 : a cool Neptune (10 Earth masses), found as a 2-day anomaly at intermediate magnification (Muraki *et al.* 2011).

Microlensing is currently the only available technique that can detect small cool planets beyond the snow line (see Fig. 1), a population complementary to the small hot planets found by the Kepler mission. Moreover, with upgraded surveys (MOA-2, OGLE-IV)

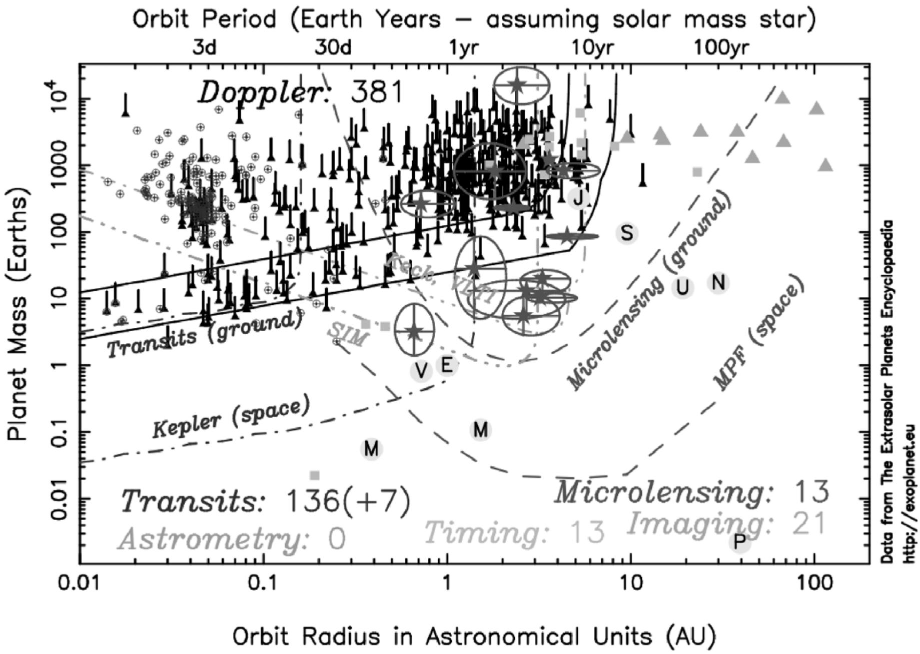

Figure 1. Exoplanets discovery space for different techniques. Different points show planets detected so far: small triangles with error bars for Doppler, circles with crosses for transit method, triangles for imaging, squares for timing and stars with error bars for microlensing. Letters in circles denote planets from the Solar System. A colour version of this figure is available on the Symposium's Website.

and consequent improvement in time-sampling of the light curves, microlensing is also sensitive to free-floating planets. The duration of an event towards the Galactic Centre provides an approximate lens mass, $M \sim M_J \ (t_{\rm E}/{\rm day})^2$. The MOA survey finds an excess of short-timescale (∼1d) events relative to predictions for mass functions for stars and brown dwarfs, interpreted as a population of unbound or distant planets, suggesting roughly 2 Jupiter masses in unbound planets per solar mass of stars (Sumi *et al.* 2011).

The Future of Microlensing. The field of microlensing has been developing for over a decade. To detect cool planets, the current strategy relies on wide-field survey telescopes to detect the events, and on follow-up networks to find and characterise anomalies. With recent MOA and OGLE upgrades, plus a new wide-field camera on the Wise Observatory 1-m telescope in Israel, the wide-field surveys may soon be delivering high-cadence quasi-continuous coverage of many events in parallel. The planned 1.6-m Korean Microlensing Telescope Network will have similar capabilities. Also promising is the deployment of 1-m robotic telescope networks with Lucky Imaging cameras (LCOGT, SONG) aiming to deliver sub-arcsecond imaging routinely in the crowded Bulge fields. These systematic ground-based surveys should deliver cool planet population statistics down to or below $M_\oplus$. In space, the European Gaia mission will soon be observing microlensing events, and the Dark Energy missions Euclid and Wfirst may also undertake microlensing surveys capable of finding hunderds of cool Earth-mass planets.

https://doi.org/10.1017/S1743921312000610 Published online by Cambridge University Press

2. Robotic Follow-Up (RS)

Responding to microlensing alerts is the most demanding of observing campaigns. The events never repeat, but last $\leqslant$few months, distributed throughout a $\sim$6 month season and must be monitored continuously for many days around the peak. Objects in the large ($\sim$1500) target list can change in importance in a matter of minutes, so new data must be reduced and re-analysed immediately in order that priorities can be reassessed. Robotic telescope facilities, distributed in longitude, offer a highly efficient way to monitor ongoing events and to respond very quickly to alerts without the overheads of a large team of manual observers. Moreover, a completely deterministic prioritisation process is desirable so that the yield of planets detected and characterised in this way can be more easily applied to understand the underlying population of planets beyond the snowline. Of course, the challenges of this approach lie in the availability of robotic telescopes over several sites, and in developing reliable software capable of executing such a dynamic observing campaign.

Las Cumbres Observatory Global Telescope Network (LCOGT). LCOGT is building a global network of robotic telescopes at six sites in both hemispheres. Each site will host a cluster of telescopes, typically 2 1-m ones plus 3 0.4-m ones. To date, 2-m telescopes are already in operation: at Faulkes Telescopes North (FTN; Hawai'i) and South (FTS; Siding Spring, Australia). The complete network will have about 12 1-m telescopes and some 2 dozen 0.4-m ones.

All telescopes of a given class will have a homogenous complement of instrumentation, including imagers (in operation), Lucky Imaging Cameras (being commissioned at the present time) and spectrographs (under development—see p. 408). Rather than allocate a given observation to a specific telescope, programmes will be coordinated across the network, allowing telescopes at other sites to take over in the event of poor weather at one location. Unlike the SONG and MiNDStEP networks, LCOGT is not dedicated to microlensing. In partnership with SUPA/St. Andrews, LCOGT's southern ring is being deployed first, with site construction underway at the Cerro Tololo Interamerican Observatory, the South African Astronomical Observatory and McDonald Observatory, while the Siding Spring site is being expanded. The aim is to have 1 1-m telescope and 2 0.4-m ones operational at CTIO and SAAO by mid-2012; the rest of the network is to be deployed between 2012–2014.

Robotic Control Systems. The RoboNet Project exploits the LCOGT network, plus the Liverpool Telescope on La Palma, to obtain photometric follow-up of high-priority microlensing events in a completely robotic way. The first step is to prioritise algorithmically the list of events active at any given time according to their sensitivity to planets. The system implements this algorithm, WebPLOP (Horne *et al.* 2009), and incorporates a publically-accessible portal at `robonet.lcogt.net`. It subscribes to the ARTEMiS (Dominik, *et al.* 2010) system for anomaly alerts, but can also receive overriding orders from operators. Web-PLOP is queried robotically about every 30 min by the Observation Control software, which receives a list of current targets, and requests observations automatically from the telescope network. It also handles the returning data, preparing them for reduction. ObsControl provides a Web-based interface too, so that team members around the world can request additional observations, and issue target-of-opportunity overrides as needed. In the final stage the data are received by the data reduction pipeline, which uses the DanDIA (Bramich, 2008) software package to perform difference image analyses. The pipeline is fully automated, including target identification, making the photometry available publicly via the Website. The software also has an on-line portal to allow team members to interact with the data reductions.

Results and Future Developments. The robotic system has successfully obtained good coverage of almost all the lensing planets discovered in recent years, including MOA-2010-BLG-0266 (Muraki *et al.* 2011), MOA-2009-BLG-0319 (Miyake *et al.* 2011) and MOA-2009-BL-0387 (Batista *et al.* 2011). Additional planetary lensing events are still being analysed.

When increased telescope resources become available in the near future, it is anticipated that more complete coverage will be provided in future seasons. The Lucky Imaging cameras that are currently being commissioned at FTN and FTS will provide high spatial resolution imaging that will resolve blends in the dense star-fields of the Galactic Bulge. The plan is to install them on all the telescopes in the 1-m network.

Figure 2. Map of LCOGT sites, including existing sites in Hawai'i and Australia, sites under construction, and possible future sites under consideration.

3. Dark Matter: Probing Galactic Structure with Microlensing (MM)

Microlensing is a powerful tool for probing the Milky-Way structure. Searches for microlensing towards the Magellanic Clouds (LMC, SMC) were originally intended to measure the optical depths through the Galactic halo in order to quantify dark matter in the form of massive compact objects. The searches towards the Galactic plane (Galactic centre and spiral arms) also enable measurements of the optical depth that is due to ordinary stars in the Galactic disk and bulge.

The microlensing optical depth up to a given source distance D_S is defined as the instantaneous probability for the line of sight of a target source to intercept a deflector's Einstein disk, that corresponds to a magnification $A > 1.34$. This probability is found to be independent of the deflectors' mass function:

$$\tau(D_S) = \frac{4\pi G D_S^2}{c^2} \int_0^1 x(1-x)\rho(x)\mathrm{d}x\,, \tag{3.1}$$

where $\rho(x)$ is the mass density of deflectors located at a distance xD_S. The *mean*

https://doi.org/10.1017/S1743921312000610 Published online by Cambridge University Press

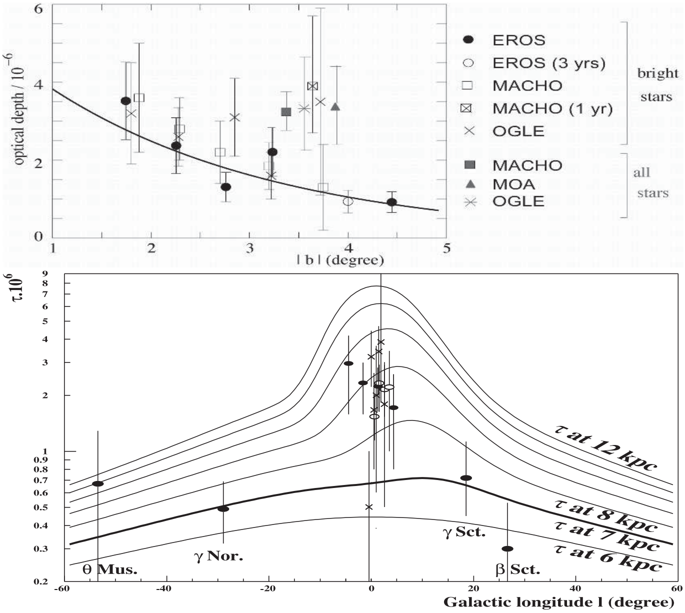

Figure 3. *Upper:* The optical depth through the Galactic plane as a function of the absolute Galactic latitude $|b|$. The line shows the fit (3.3). *Lower:* The optical depth at $< b >= -2.5°$ as a function of Galactic longitude; MACHO: open circles, EROS: filled circles, OGLE: crosses. The lines show the predicted optical depths as a function of latitude at 6, 7 (thick line), 8, 9, 10, 11 and 12 kpc [Rahal 2009], The measured optical depths around $l = 0°$ are compatible with the expected value at 8.5 kpc.

optical depth towards a given population of sources defined by the distance distribution $\mathrm{d}n_S(D_S)/\mathrm{d}D_S$ is defined as:

$$< \tau >= \int_0^\infty \frac{\mathrm{d}n_S(D_S)}{\mathrm{d}D_S} \tau(D_S) D_S^2 \, \mathrm{d}D_S \ \Big/ \int_0^\infty \frac{\mathrm{d}n_S(D_S)}{\mathrm{d}D_S} D_S^2 \, \mathrm{d}D_S . \tag{3.2}$$

The estimate of $< \tau >$ is obtained from the distribution of the characteristic times t_E of the detected events, and needs the knowledge of the detection efficiency as a function of t_E, the most delicate aspect of this measurement. The rest of this review focusses on the results from the microlensing surveys towards targets with resolved stars, EROS, MACHO, OGLE and MOA.

Results towards the Galactic plane. More than 4000 events have been detected towards the Galactic bulge (but only a fraction have been used to estimate optical depths under controlled efficiency), and 27 towards the Galactic Spiral Arms (22 used for optical depth determination). The optical depth measurements are summarized in Fig. 3. The variation with the latitude deduced from the largest sample (EROS, Hamadache *et al.* 2006) is fitted well by:

$$\tau/10^{-6} = (1.62 \pm 0.23) \exp[-a(|b| - 3°)], \text{ with } a = (0.43 \pm 0.16) \text{ deg}^{-1} . \tag{3.3}$$

This fit agrees with the results of MACHO (Popowski *et al.* 2005) and OGLE (Sumi *et al.* 2006) and with the Galactic models of Evans & Belokurov (2002) and Bissantz *et al.* (1997). There is also a satisfactory agreement between the measured optical depths towards the Galactic spiral arms and the model expectations, and there is no indication for a population of hidden compact objects in the disk.

Interpreting the Magellanic cloud surveys: halo versus local structures. The main result from the LMC/SMC surveys is that compact objects of mass within a $[10^{-7}, 10] \times m_\odot$ interval are not a major component of the hidden Galactic mass (Fig. 4).

The considerable differences between the EROS, MACHO and OGLE data sets may explain the apparent MACHO vs EROS/OGLE discrepancies: MACHO used fainter stars

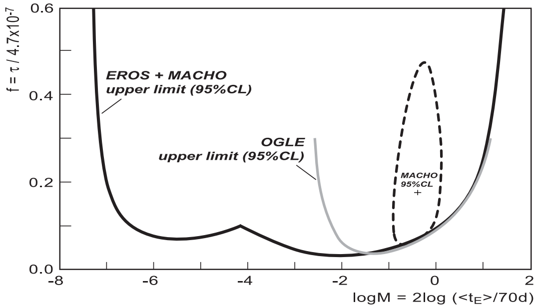

Figure 4. Constraints on the fraction f of the standard spherical Galactic halo made of massive compact objects as a function of their mass M. The solid line shows the combined EROS+MACHO upper limit [Moniez 2010]. The OGLE upper limit [Wyrzykowski *et al.* 2011] is shown in grey. The closed domain is the 95% CL contour for the f value claimed by MACHO (Alcock *et al.* 2000).

in denser fields (1.2×10^7 stars over $14\,\mathrm{deg}^2$) than EROS and OGLE (0.7×10^7 stars over $90\,\mathrm{deg}^2$). The faint source stars also made the efficiency estimates more complicated owing to larger blending effects. The observational results at their face value indicates that the hypothesis of an optical depth dominated by the Galactic halo—almost uniform through all the monitored LMC fields and 1.4 times larger towards SMC—is wrong, because it cannot explain the EROS–MACHO–OGLE differences nor the LMC–SMC differences. That said, the apparent discrepancy between the surveys can be understood by considering local structures inducing self-lensing; such structures (populations of foreground lenses as well as of background sources (Alcock *et al.* 2000) may be responsible for the variability of the optical depth with the monitored zones.

Conclusion and perspectives.
The hypothesis that compact objects make a substantial contribution to a standard halo is now clearly excluded. Observations towards both the SMC and the spiral arms find that compact objects belonging to a flattened halo or a thick disk are also scarce. Whether there is a small dark-matter component in the form of compact objects is still an open question that will be addressed by the infrared VVV project (using VISTA facility) and the LSST project, possibly with contributions from space missions like Gaia.

4. Serendipitous Science with Microlensing Data (ŁW)

This section contains a brief, subjective review of recent highlights of serendipitous science from the vast time-domain data collected by Ogle, a long-term microlensing survey which was initiated in 1992 by Bohdan Paczyński (Princeton) and Andrzej Udalski (Warsaw). Since 1996 Ogle has used a dedicated 1.3-m telescope at Las Campanas Observatory, Chile (Udalski *et al.* 2008). In 2010 March it entered into its fourth phase, when the detector was upgraded to a 32-chip mosaic CCD camera covering 1.4 deg^2.

Photometric maps. Since microlensing events are predominantly being found in dense sky areas, OGLE regularly observes hundreds of square degrees towards the Galactic Bulge, Magellanic Clouds and Galactic Disk. Superb quality observations in I and V give rise to detailed colour-magnitude diagrams for the observed fields (Udalski *et al.* 2008; Szymański *et al.* 2010; Szymański *et al.* 2011). All the photometric data are made available through OGLE's Webpage†. They are useful in tasks such as mapping interstellar extinction, studying stellar populations, or studying the Bulge and Magellanic Cloud structures using stars in the Red Clump and the Tip of the Red Giant Branch.

† `http://ogle.astrouw.edu.pl`

Variable stars. A natural by-product of long-term photometric monitoring is numerous discoveries of variable stars. The catalogue based only on OGLE-III data from 2001–2009 already consists of 13 parts, each devoted to a different type of variable. The number of catalogued variables exceeds all known catalogues to date, e.g., 24,906 RR Lyræ stars found in the LMC alone (Soszyński *et al.* 2009) and 16,836 in the Bulge (Soszyński *et al.* 2011). Vast numbers of variable stars enable detailed statistical studies of those populations, but also reveal rare examples of peculiar objects, including RR Lyraes or Cepheids in eclipsing systems (Pietrzynski *et al.* 2010), or R CrB-type stars (Soszyński *et al.* 2009).

Pulsating variables and period-luminosity relation. The long time-base-line of observations enables the detection of periodic variable stars with periods ranging from hours to years. The well-known period-luminosity relation for classical Cepheids was extended by OGLE variables in all directions, with δ Scuti and RR Lyræ stars at the short-period end and OSARGS, Miras and LSPs at the long-period end (see Soszyński *et al.* 2007; Poleski *et al.* 2010). The large statistical sample of all pulsators provided by OGLE is supporting detailed theoretical studies of those stars, and is also being used for measurements of distance.

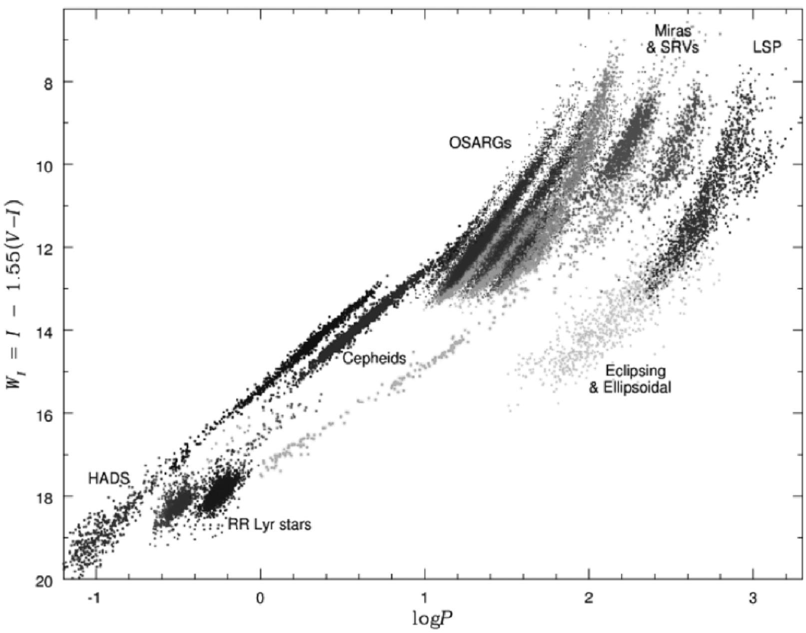

Figure 5. OGLE's variable stars period-luminosity relation. A colour version of this figure is available in the on-line edition.

Transiting planets. Ogle was among the first to conduct a massive search for transiting planets. Thanks to the milli-mag precision of its photometry, Ogle found a few dozen candidates (e.g. Udalski *et al.* 2004), among which about a dozen were confirmed by radial-velocity observations.

Miscellaneous. Owing to the long time-span between observations of the same regions of the sky, it is possible to measure the proper motions of the fastest stars (Soszyński *et al.* 2002), of asteroids and of Kuiper Belt Objects. Continuing observations are also revealing numerous supernovæ behind the Magellanic Clouds (Udalski 2003), as well as classical and dwarf novæ. Among other highlights is the recent capture of a nova explosion following an apparent merger of the components of a contact binary (Tylenda *et al.* 2011).

Acknowledgements

KH and RS acknowledge Qatar Foundation support through QNRF Grant NPRP-09-476-1-78. ŁW and the OGLE project acknowledge support of European Community's FP7 ERC Grant no. 246678.

References

Alcock, C., *et al.*, 2000, *ApJ*, 542, 281
Alcock, C., *et al.*, 2000, *ApJ*, 552, 582
Batista, V., *et al.* 2011, *ApJ*, 529, A102.
Beaulieu, J.-P., *et al.* 2006, *Nature*, 439, 437
Belokurov, V., Evans, N. W., & Le Du, Y. 2003, *MNRAS*, 341, 1373
Bissantz, N., Englmaier, P., Binney, J., & Gerhard, 0 .E., 1997, *MNRAS*, 289, 651
Bramich, D. 2008, *MNRAS*, 386, 77.
Dominik, M., *et al.* 2010, *AN*, 331, 671.
Evans, N. W. & Belokurov, V., 2002, *ApJ*, 567, L119
Gaudi, B. S., *et al.* 2008, *Science*, 319, 927
Hamadache, C., *et al.*, 2006, *A&A*, 454, 185
Horne, K., *et al.* 2009, *MNRAS*, 396, 2087.
Miyake, N., *et al.* 2011, *ApJ*, 728, 120.
Moniez, M., 2010, *GRG*, 42, 2047
Muraki, Y., *et al.* 2011, *ApJ*, 741, 22
Pietrzynski, G. *et al.* 2010, *Nature*, 468, 542
Poleski, R,. *et al.* 2010, *AcA*, 60, 1
Popowski, P., *et al.*, 2005, *ApJ*, 631, 879
Rahal, Y. R., 2009, *A&A*, 500, 1027
Sumi, T., *et al.* (OGLE collaboration), 2006, *ApJ*, 636, 240
Sumi, T., *et al.* 2011, *Nature*, 473, 349
Soszyński, I., *et al.* 2002, *AcA*, 52, 143
Soszyński, I., *et al.* 2007, *AcA*, 57, 201
Soszyński, I., *et al.* 2009, *AcA*, 59, 1
Soszyński, I., *et al.* 2009, *AcA*, 59, 335
Soszyński, I., *et al.* 2011, *AcA*, 61, 1
Szymański, M. K., *et al.* 2010, *AcA*, 60, 295
Szymański, M. K., *et al.* 2011, *AcA*, 61, 83
Tylenda, R., *et al.* 2011, *A&A*, 528, A114
Udalski, A. 2003, *AcA*, 53, 291
Udalski, A. *et al.* 2004, *AcA*, 54, 313
Udalski, A., *et al.* 2005, *ApJ*, 628, L109
Udalski, A. *et al.* 2008, *AcA*, 58, 69
Udalski, A. *et al.* 2008, *AcA*, 58, 329
Wyrzykowski, Ł. *et al.*, 2011, *MNRAS*, 416, 2949